Inorg. Chem. **2005**, *44*, 1966–1972

Inorganic Chemistry
Article

Effects of the Intramolecular NH···S Hydrogen Bond in Mononuclear Platinum(II) and Palladium(II) Complexes with 2,2′-Bipyridine and Benzenethiol Derivatives

Masahiro Kato, Taka-aki Okamura, Hitoshi Yamamoto, and Norikazu Ueyama*

Department of Macromolecular Science, Graduate School of Science, Osaka University, Toyonaka, Osaka 560-0043 Japan

Received July 22, 2004

A series of complexes, [M(bpy)(SAr)$_2$] (M = platinum(II) or palladium(II), bpy = 2,2′-bipyridine, SAr = 2- or 4-(acylamino)benzenethiolate, or 2-(alkylcarbamoyl)benzenethiolate), were synthesized and characterized on the basis of ^{1}H NMR, IR, and electrochemical properties. The structures of [Pt(bpy)(S-2-Ph$_3$CCONHC$_6$H$_4$)$_2$] (**1**) and [Pt(bpy)(S-2-*t*-BuNHCOC$_6$H$_4$)$_2$] (**3**) were determined by X-ray analysis. The complexes have intramolecular NH···S hydrogen bonds between the amide NH group and the sulfur atom. A weak NH···S hydrogen bond in these complexes and [Pd(bpy)(S-2-Ph$_3$CCONHC$_6$H$_4$)$_2$] (**4**) is detected from the ^{1}H NMR spectra and the IR spectra in chloroform and in the solid state. [Pt(bpy)(S-2-Ph$_3$CCONHC$_6$H$_4$)$_2$] (**1**) exhibits a remarkably high-energy-shifted lowest-energy band in UV–visible spectra and has a positively shifted oxidation potential. The blue-shift of 42 nm and the positive shift of +0.24 V, as compared to those of [Pt(bpy)(SC$_6$H$_5$)$_2$], are due to the effect of the NH···S hydrogen bond.

Introduction

Platinum(II) diimine complexes Pt(diimine)L$_2$ (L = thiolate,[1−8] acetylide,[9−14] phenyl,[15] and cyanide;[16−18] diimine = bipyridine, phenanthroline, and derivatives) have been of increasing interest recently as chromophores in the light-chemical energy conversion. These platinum(II) diimine complexes feature long-lived charge-separated excited states. The description of the low-energy excited states in this class of complexes first requires the assignment of their frontier orbitals, in particular, the HOMO and LUMO. The lowest excited state in platinum(II)−diimine dithiolate complexes was assigned as the charge transfer from the HOMO of mixed S(pπ)−Pt(dπ) to the LUMO of diimine(π*) character.[6,8] In addition, for a flexible bis-thiolate complex, Pt(bpy)-(4-X−C$_6$F$_4$S)$_2$, it is reported that the HOMO is composed of thiolate(π)/S(p)/Pt(d) orbitals and the LUMO is largely localized on the π* (diimine) orbitals.[2,7] Consequently, its

---

* Author to whom correspondence should be addressed. E-mail: ueyama@chem.sci.osaka-u.ac.jp.

(1) Hissler, M.; McGarrah, J. E.; Connick, W. B.; Geiger, D. K.; Cummings, S. D.; Eisenberg, R. *Coord. Chem. Rev.* **2000**, *208*, 115−137.
(2) Weinstein, J. A.; Blake, A. J.; Davies, E. S.; Davis, A. L.; George, M. W.; Grills, D. C.; Lileev, I. V.; Maksimov, A. M.; Matousek, P.; Mel'nikov, M. Y.; Parker, A. W.; Platonov, V. E.; Towrie, M.; Wilson, C.; Zheligovskaya, N. N. *Inorg. Chem.* **2003**, *42*, 7077−7085.
(3) Geary, E. A. M.; Hirata, N.; Clifford, J.; Durrant, J. R.; Parsons, S.; Dawson, A.; Yellowlees, L. J.; Robertson, N. *Dalton Trans.* **2003**, 3757−3762.
(4) Islam, A.; Sugihara, H.; Hara, K.; Singh, L. P.; Katoh, R.; Yanagida, M.; Takahashi, Y.; Murata, S.; Arakawa, H.; Fujihashi, G. *Inorg. Chem.* **2001**, *40*, 5371−5380.
(5) Smucker, B. W.; Hudson, J. M.; Omary, M. A.; Dunbar, K. R. *Inorg. Chem.* **2003**, *42*, 4714−4723.
(6) Zuleta, J. A.; Bevilacqua, J. M.; Proserpio, D. M.; Harvey, P. D.; Eisenberg, R. *Inorg. Chem.* **1992**, *31*, 2396−2404.
(7) Weinstein, J. A.; Zheligovskaya, N. N.; Mel'nikov, M. Y.; Hartl, F. *J. Chem. Soc., Dalton Trans.* **1998**, 2459−2466.
(8) Cummings, S. D.; Eisenberg, R. *J. Am. Chem. Soc.* **1996**, *118*, 1949−1960.
(9) McGarrah, J. E.; Eisenberg, R. *Inorg. Chem.* **2003**, *42*, 4355−4365.
(10) Wadas, T. J.; Lachicotte, R. J.; Eisenberg, R. *Inorg. Chem.* **2003**, *42*, 3772−3778.
(11) Pomestchenko, I. E.; Luman, C. R.; Hissler, M.; Ziessel, R.; Castellano, F. N. *Inorg. Chem.* **2003**, *42*, 1394−1396.
(12) Whittle, C. E.; Weinstein, J. A.; George, M. W.; Schanze, K. S. *Inorg. Chem.* **2001**, *40*, 4053−4062.
(13) Kang, Y.; Lee, J.; Song, D.; Wang, S. *Dalton Trans.* **2003**, 3493−3499.
(14) Fleeman, W. L.; Connick, W. B. *Comments Inorg. Chem.* **2002**, *23*, 205−230.
(15) Klein, A.; van Slageren, J.; Zalis, S. *Eur. J. Inorg. Chem.* **2003**, 1917−1928.
(16) Pettijohn, C. N.; Jochnowitz, E. B.; Chuong, B.; Nagle, J. K.; Vogler, A. *Coord. Chem. Rev.* **1998**, *171*, 85−92.
(17) Chan, C. W.; Cheng, L. K.; Che, C. M. *Coord. Chem. Rev.* **1994**, *132*, 87−97.
(18) Kuimova, M. K.; Mel'nikov, M. Y.; Weinstein, J. A.; George, M. W. *J. Chem. Soc., Dalton Trans.* **2002**, 2857−2861.

10.1021/ic0490167 CCC: $30.25

energies are strongly dependent on the nature of the ligands coordinated to platinum. More electron-withdrawing ligands on platinum cause the bands to move to a higher energy level.

Previously, we reported that the NH···S hydrogen bond contributes to the positive shift in the redox potential in benzenethiolate or Cys-containing oligopeptide Fe(II) complexes[19−26] as models of the Fe center of iron−sulfur proteins and Fe(III) complexes[27−31] as models of the Fe(III) porphinate proteins such as P-450 and chloroperoxidase. The NH···S hydrogen bond has been found to shift the redox potential in $[\mathrm{Mo^{V}O}(2\text{-(acetylamino)benzenethiolate})_4]^-$.[32] Thus, NH···S hydrogen bonding can conceivably produce a positive shift in the redox potential in any metal thiolate complex. The presence of such hydrogen bonds in Fe(II),[19,21,23,26] Fe(III),[27−31] Ga(III),[30,31,33] Mo(V),[32] Mo(IV), Co(II),[21] Cu(I),[34] Cd(II), and Hg(II)[35] complexes has already been reported.

This paper describes the presence of the intramolecular NH···S hydrogen bond in platinum(II) diimine complexes containing bis(benzenethiolate) derivatives, 2-(acylamino)benzenethiolate, 4-(acylamino)benzenethiolate, and 2-(alkylcarbamoyl)benzenethiolate and related palladium(II) complexes, and it also describes the influence of the hydrogen bond in the sulfur atom coordinated to platinum on the UV−visible spectra and the electrochemical properties of platinum(II) diimine complexes (Chart 1).

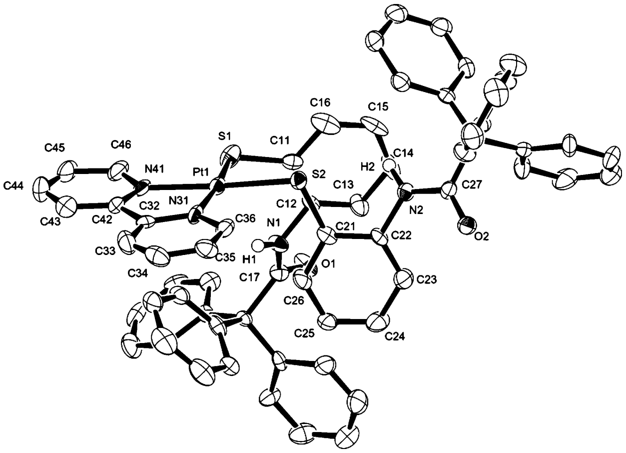

Figure 1. Crystal structure of $[\mathrm{Pt(bpy)(S\text{-}2\text{-}Ph_3CCONHC_6H_4)_2}]$ (**1**). Thermal ellipsoids are drawn at 50% probability. The hydrogen atoms except for the amide proton have been omitted for clarity.

Chart 1

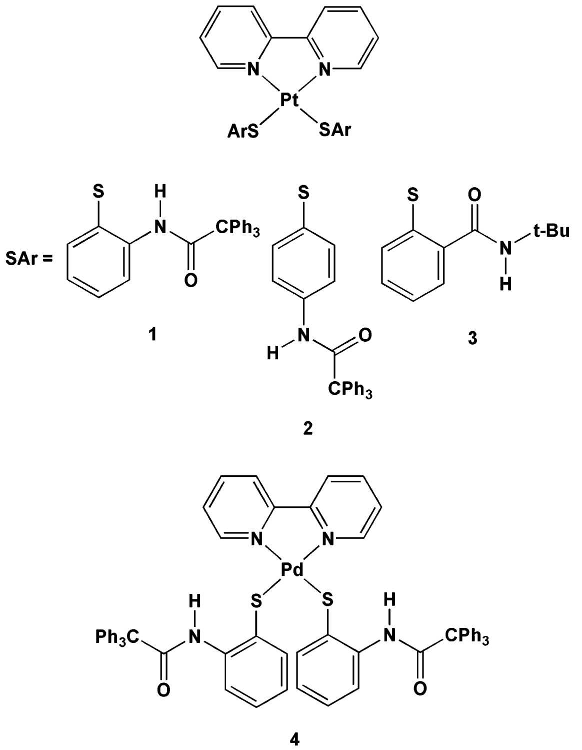

Results and Discussion

Crystal Structures of $[\mathrm{Pt(bpy)(S\text{-}2\text{-}Ph_3CCONHC_6H_4)_2}]$ (1) and [Pt(bpy)(S-2-*t*-BuNHCOC$_6$H$_4$)$_2$] (3). Complexes **1** and **3** crystallized in the $P2_1/n$ and $P2/c$ space groups, respectively. ORTEP views of **1** and **3** are shown in Figures1 and 2, respectively. Selected bond distances and bond angles for both complexes are listed in Table 1. Both complexes show that the expected Pt coordination geometry is approximately square planar, with one 2,2′-bipyridine and two thiophenolate ligands binding to the Pt(II) center. One of the two thiophenol rings in **3** is disordered with Pt(1)−S(2)−C(21)−C(22) dihedral angles of 177.6(5)° or −155.2(5)°. The angle between the planes of the two thiophenol rings coordinated to platinum in **1** is 165.2(2)°, and the two thiophenol rings of **1** show intramolecular $\pi-\pi$ stacking with C(11)···C(21) = 3.49 Å and C(12)···C(21) = 3.52 Å. The angles between the thiophenol rings and the PtS$_2$ plane are 82.0(1)° and 86.0(1)°, and the structure of complex **1** is analogous to Pt(bpy)(4-CN−C$_6$F$_4$S)$_2$.[2] In contrast, the two thiophenol rings in **3** are in an anti configuration, thus

---

(19) Ueyama, N.; Okamura, T.; Nakamura, A. *J. Chem. Soc., Chem. Commun.* **1992**, 1019−1020.

(20) Ueyama, N.; Yamada, Y.; Okamura, T.; Kimura, S.; Nakamura, A. *Inorg. Chem.* **1996**, *35*, 6473−6484.

(21) Okamura, T.; Takamizawa, S.; Ueyama, N.; Nakamura, A. *Inorg. Chem.* **1998**, *37*, 18−28.

(22) Ueyama, N.; Terakawa, T.; Nakata, M.; Nakamura, A. *J. Am. Chem. Soc.* **1983**, *105*, 7098−7102.

(23) Sun, W. Y.; Ueyama, N.; Nakamura, A. *Inorg. Chem.* **1991**, *30*, 4026−4031.

(24) Ohno, R.; Ueyama, N.; Nakamura, A. *Inorg. Chem.* **1991**, *30*, 4887−4891.

(25) Ueyama, N.; Kajiwara, A.; Terakawa, T.; Ueno, S.; Nakamura, A. *Inorg. Chem.* **1985**, *24*, 4700−4704.

(26) Ueyama, N.; Nakata, M.; Fuji, M.; Terakawa, T.; Nakamura, A. *Inorg. Chem.* **1985**, *24*, 2190−2196.

(27) Ueyama, N.; Nishikawa, N.; Yamada, Y.; Okamura, T.; Oka, S.; Sakurai, H.; Nakamura, A. *Inorg. Chem.* **1998**, *37*, 2415−2421.

(28) Ueyama, N.; Nishikawa, N.; Yamada, Y.; Okamura, T.; Nakamura, A. *Inorg. Chim. Acta* **1998**, *283*, 91−97.

(29) Ueyama, N.; Nishikawa, N.; Yamada, Y.; Okamura, T.; Nakamura, A. *J. Am. Chem. Soc.* **1996**, *118*, 12826−12827.

(30) Ueno, T.; Kousumi, Y.; Yoshizawa-Kumagaye, K.; Nakajima, K.; Ueyama, N.; Okamura, T.; Nakamura, A. *J. Am. Chem. Soc.* **1998**, *120*, 12264−12273.

(31) Ueno, T.; Nishikawa, N.; Moriyama, S.; Adachi, S.; Lee, K.; Okamura, T.; Ueyama, N.; Nakamura, A. *Inorg. Chem.* **1999**, *38*, 1199−1210.

(32) Ueyama, N.; Okamura, T.; Nakamura, A. *J. Am. Chem. Soc.* **1992**, *114*, 8129−8137.

(33) Okamura, T.; Nishikawa, N.; Ueyama, N.; Nakamura, A. *Chem. Lett.* **1998**, 199−200.

(34) Okamura, T.; Ueyama, N.; Nakamura, A.; Ainscough, E. W.; Brodie, A. M.; Waters, J. M. *J. Chem. Soc., Chem. Commun.* **1993**, 1658−1660.

(35) Ueyama, N.; Taniuchi, K.; Okamura, T.; Nakamura, A.; Maeda, H.; Emura, S. *Inorg. Chem.* **1996**, *35*, 1945−1951.

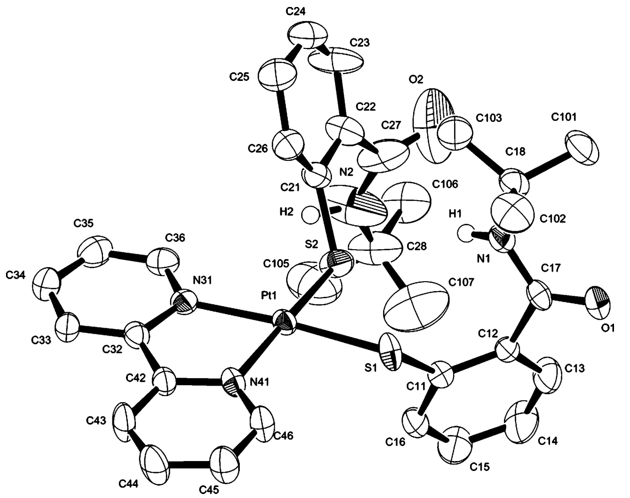

Figure 2. Crystal structure of [Pt(bpy)(S-2-*t*-BuNHCOC$_6$H$_4$)$_2$] (**3**). Thermal ellipsoids are drawn at 50% probability. The hydrogen atoms except for the amide proton have been omitted for clarity. The figure depicts only one of two disordered sites corresponding to the 50:50 disordered thiophenolate ligand.

Table 1. Selected Bond Distances (Å), Intramolecular NH···S Contacts (Å), and Bond Angles (deg) of [Pt(bpy)(S-2-Ph$_3$CCONHC$_6$H$_4$)$_2$] (**1**) and [Pt(bpy)(S-2-*t*-BuNHCOC$_6$H$_4$)$_2$] (**3**)

	1	3
Pt(1)−S(1)	2.284(1)	2.283(3)
Pt(1)−S(2)	2.289(1)	2.285(3)
Pt(1)−N(31)	2.045(3)	2.067(3)
Pt(1)−N(41)	2.071(4)	2.059(4)
N(1)···S(1)	3.020(4)	3.161(6)
N(2)···S(2)	2.949(4)	3.01(2), 3.10(2)[a]
Pt(1)−S(1)−C(11)	111.9(1)	107.3(1)
Pt(1)−S(2)−C(21)	107.3(2)	111.6(1)
S(1)−Pt(1)−S(2)	93.79(4)	88.4(1)
N(41)−Pt(1)−S(1)	92.8(1)	94.2(1)
N(31)−Pt(1)−S(2)	94.6(1)	98.2(1)
N(31)−Pt(1)−N(41)	78.9(1)	79.3(2)
Pt(1)−S(1)−C(11)−C(12)	91.7(4)	133.0(2)
Pt(1)−S(2)−C(21)−C(22)	163.2(3)	177.6(5), −155.2(5)[a]

[a] Atoms N(2) and C(22) are disordered.

eliminating the possibility of intramolecular $\pi-\pi$ stacking as observed in **1**, and are nearly perpendicular to the PtS$_2$ planes (dihedral angle = 74°, 109°). The dihedral angle between the amide groups and the thiophenol ring for **1**, C(17)−N(1)−C(12)−C(13), is −38.4(6)° and another ring, C(27)−N(2)−C(22)−C(23), is −42.5(6)°, and that between the carbamoyl groups and the thiophenol ring for **3**, N(1)−C(17)−C(12)−C(11), is −49.9(4)° and another disordered ring, N(2)−C(27)−C(22)−C(21), is 48(1)° or −48(1)°, values that are not favorable for spreading the π-conjugated systems. Accordingly, we carried out computations with Gaussian03 (B3LYP/LanL2DZ) on the energy changes for complex **1** by altering the angle between the planes of the amide group and thiophenol ring. The result of our computations shows that the structure of **1** (dihedral angle = 38.4° and 42.5°) is stabilized by ca. 2.0 kcal/mol^{-1} relative to the model structure in which these dihedral angles are 0°. The amide NH groups for **1** are directed to form an intramolecular NH···S hydrogen bond contained in a five-membered ring and a six-membered ring for **3**. The distances between the nitrogen atom and the sulfur atom are 3.020(4) Å (N(1)−S(1)), 2.949(4) Å (N(2)−S(2)) for **1** and 3.161(6) Å (N(1)−S(1)), 3.10(2) Å or 3.01(2) Å (N(2)−S(2)) for **3** (Table 1). In addition, the S(1)···H(1) and S(2)···H(2) distances in complex **1** are 2.65 and 2.60 Å, whereas the S(1)···H(1), S(2)···H(2), and S(2)···H(2B) distances in complex **3** are 2.96, 2.83, and 2.51 Å, respectively. The previous structural analyses in metalloproteins and model complexes suggest that the distances forming an NH···S hydrogen bond are ca. 3.0−3.5 Å at N···S, and ca. 2.3−2.8 Å at S···H.[27,28,31,36−39] Therefore, complex **1** has two equal NH···S hydrogen bonds, and complex **3** has two distinct NH···S hydrogen bonds confirmed by the IR spectra in solid, as described later. The crystal structure of the corresponding thiol compound, 2-*t*-BuNHCOC$_6$H$_4$SH, shows the formation of the intramolecular SH···O=C hydrogen bond, not that of the intramolecular NH···S hydrogen bond.[40] Consequently, this finding suggests that the coordination of the sulfur atom to platinum results in the rotation of the amide plane and the formation of the intramolecular NH···S hydrogen bond in complex **3**.

^{1}H NMR Spectra. The amide NH signal in 2-Ph$_3$CCONHC$_6$H$_4$SH appears at 8.28 ppm of normal chemical shift. This signal in (NEt$_4$$^+$)(2-Ph$_3$CCONHC$_6H_4S^-$) is shifted downfield by 2.04 ppm to 10.32 ppm, due to the formation of an intramolecular NH···S hydrogen bond. The amide NH signal in **1** appears at 8.74 ppm and shifts downfield by 0.46 ppm as compared to that of the thiol form. This small shift in **1** as compared to that of the thiolate anion suggests that the intramolecular NH···S hydrogen bond is weak. It was previously revealed that the increase of covalency between metal and thiolate decreases the electron density of S coordinated to metal and weakens the intramolecular NH···S hydrogen bond.[35] The small shift in **1** is ascribed to the lower acidity of amide NH through the formation of hydrogen bond as compared to the thiolate anion. Consequently, these findings predict that the intramolecular NH···S hydrogen bond between the sulfur atom binding to Pt(II) and the amide NH is weaker than that in the thiolate anion form, (NEt$_4$$^+$)(2-Ph$_3$CCONHC$_6H_4S^-$). This prediction is supported by the IR spectra in solution, as described later. The chemical shifts of the amide NH for other complexes are summarized in Table 2. The amide NH signal in [Pt(bpy)(S-2-*t*-BuNHCOC$_6$H$_4$)$_2$] (**3**) shifts downfield by 1.62 ppm as compared to the corresponding thiol compound. This shift is smaller than that in the thiolate anion (6.47 ppm),[40] and complex **3** also forms a weak intramolecular NH···S hydrogen bond. The amide NH signal in a palladium complex, [Pd(bpy)(S-2-Ph$_3$CCONHC$_6$H$_4$)$_2$] (**4**), which has the same coordination structure as platinum complexes, shifts

---

(36) Adman, E.; Watenpaugh, K. D.; Jensen, L. H. *Proc. Natl. Acad. Sci. U.S.A.* **1975**, *72*, 4854−4858.

(37) Watenpaugh, K. D.; Sieker, L. C.; Jensen, L. H. *J. Mol. Biol.* **1979**, *131*, 509−522.

(38) Baker, E. N. *J. Mol. Biol.* **1988**, *203*, 1071−1095.

(39) Kissinger, C. R.; Sieker, L. C.; Adman, E. T.; Jensen, L. H. *J. Mol. Biol.* **1991**, *219*, 693−715.

(40) Kato, M.; Kojima, K.; Inohara, M.; Okamura, T.; Yamamoto, H.; Ueyama, N., submitted for publication.

Table 2. Chemical Shifts (ppm) and Temperature Coefficients (ppb/K) of Amide NHs of M(bpy)(bis)thiolates (M = Pt^{II}, Pd^{II}) Complexes and Related Compounds in Chloroform-d_1 and Acetonitrile-d_3 (10 mM)

compound	in chloroform-d_1[a]	in acetonitrile-d_3[a]
$[Pt(bpy)(S\text{-}2\text{-}Ph_3CCONHC_6H_4)_2]$ (**1**)	8.74/0.8	8.84/0.0
$[Pt(bpy)(S\text{-}4\text{-}Ph_3CCONHC_6H_4)_2]$ (**2**)	[b]	7.55/−4.0[c]
$[Pt(bpy)(S\text{-}2\text{-}t\text{-}BuNHCOC_6H_4)_2]$ (**3**)	7.40/−1.3	7.47/−0.7
$[Pd(bpy)(S\text{-}2\text{-}Ph_3CCONHC_6H_4)_2]$ (**4**)	8.75/1.1	8.91/0.0
$2\text{-}Ph_3CCONHC_6H_4SH$	8.28/−0.7	8.67/−8.2
$(NEt_4^+)(2\text{-}Ph_3CCONHC_6H_4S^-)$	10.32/−0.7	10.72/−0.5
$2\text{-}t\text{-}BuNHCOC_6H_4SH$	5.78/−2.0	6.78/−9.0
$(NEt_4^+)(2\text{-}t\text{-}BuNHCOC_6H_4S^-)$	12.25/−3.1	12.72/−1.2

[a] Chemical shift [ppm]/temperature coefficient [ppb/K]. [b] The amide signal is not detected to overlap with the signal of chloroform or triphenyl group. [c] Complex concentration ≈ 1 mM.

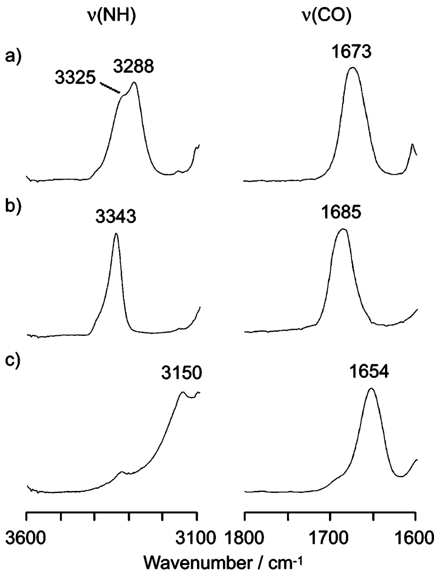

Figure 3. IR spectra of (a) $[Pt(bpy)(S\text{-}2\text{-}Ph_3CCONHC_6H_4)_2]$ (**1**), (b) $2\text{-}Ph_3CCONHC_6H_4SH$, and (c) $(NEt_4^+)(2\text{-}Ph_3CCONHC_6H_4S^-)$ in chloroform.

downfield by 0.47 ppm as compared to that of the thiol compound. This shift value is almost the same as that of the corresponding platinum complex, thus indicating that the palladium complex **4** forms the weak intramolecular NH···S hydrogen bond as well as the platinum complex **1**.

The temperature coefficients of the amide NH ^1H NMR signals in platinum complexes **1** and **3**, the palladium complex **4**, and the corresponding thiol and thiolate anion compounds are summarized in Table 2. The temperature coefficients of the amide NH signals in the thiol compounds $2\text{-}Ph_3CCONHC_6H_4SH$ and $2\text{-}t\text{-}BuNHCOC_6H_4SH$ are −0.7 and −2.0 ppb/K in chloroform-d_1 and −8.2 and −9.0 ppb/K in acetonitrile-d_3, respectively. On the other hand, those in the thiolate anion compounds $(NEt_4^+)(2\text{-}Ph_3CCONHC_6H_4S^-)$ and $(NEt_4^+)(2\text{-}t\text{-}BuNHCOC_6H_4S^-)$ are −0.7 and −3.1 ppb/K in chloroform-d_1 and −0.5 and −1.2 ppb/K in acetonitrile-d_3, respectively. The temperature coefficients of the amide signal in the thiolate anion compounds are very small as compared to those of the thiol compounds in acetonitrile-d_3. The observation of the small temperature coefficients has been established for the presence of the intramolecular NH···O═C hydrogen bond in peptides.[41−43] Obviously, the amide NH's in the thiolate anion compounds are involved in an intramolecular hydrogen bond like the NH···S hydrogen bond. The temperature coefficients of the amide NH signals in **1**, **3**, and **4** are 0.8, −1.3, and 1.1 ppb/K in chloroform-d_1 and 0.0, −0.7, and 0.0 ppb/K in acetonitrile-d_3, respectively. In contrast, the value in **2** without the intramolecular NH···S hydrogen bond is −4.0 ppb/K in acetonitrile-d_3. Consequently, the small temperature coefficients in complexes **1**, **3**, and **4** as compared to complex **2** suggest the formation of the intramolecular NH···S hydrogen bond.

IR Spectra in Solution and in the Solid State. The presence of an NH···S hydrogen bond was established by IR spectroscopy. Figure 3 shows the IR spectra of $[Pt(bpy)(S\text{-}2\text{-}Ph_3CCONHC_6H_4)_2]$ (**1**) and the corresponding thiol and thiolate anion compounds, $2\text{-}Ph_3CCONHC_6H_4SH$ and $(NEt_4^+)(2\text{-}Ph_3CCONHC_6H_4S^-)$, in chloroform-$d_1$. $2\text{-}Ph_3CCONHC_6H_4SH$ exhibits a free NH band at 3343 cm^{-1} and a free CO band at 1685 cm^{-1}. The thiolate anion compound, $(NEt_4^+)(2\text{-}Ph_3CCONHC_6H_4S^-)$, exhibits a broad NH band at 3150 cm^{-1} and CO band at 1654 cm^{-1}. This large $\Delta\nu$(NH) value (−193 cm^{-1}) for the thiolate anion compound as compared to that of the thiol compound is ascribed to the intramolecular NH···S hydrogen bond and is detected by the formation of the NH···O hydrogen bond in the corresponding carboxylate anion compounds.[44] Complex **1** exhibits two NH bands at 3288 and 3325 cm^{-1} and a CO band at 1673 cm^{-1}, as shown in Figure 3a. The $\Delta\nu$(NH) for **1** can be estimated to be −55 and −18 cm^{-1} when the stretching of the free NH in the thiol state, $2\text{-}Ph_3CCONHC_6H_4SH$, is employed as a standard. Table 3 lists the IR data in the amide region ν(NH) and ν(C═O) bands for the other platinum and palladium complexes, free ν(NH) and ν(C═O) bands of the corresponding thiol compounds, and the shift values. The amide ν(NH) values in $[Pt(bpy)(S\text{-}2\text{-}t\text{-}BuNHCOC_6H_4)_2]$ (**3**) and $[Pd(bpy)(S\text{-}2\text{-}Ph_3CCONHC_6H_4)_2]$ (**4**) were observed at 3305 and 3281 cm^{-1} by a shift of −126 and −62 cm^{-1}, respectively, as compared to the corresponding thiol compounds. The corresponding $\Delta\nu$(C═O) shifts are somewhat small (−22, −10, and −13 cm^{-1}) due to the free state of the amide C═O group. The combined data indicate the presence of the intramolecular NH···S hydrogen bond in complexes **1**, **3**, and **4**. On the other hand, $[Pt(bpy)(S\text{-}4\text{-}Ph_3CCONHC_6H_4)_2]$ (**2**) and the corresponding thiol and thiolate anion compounds, $4\text{-}Ph_3CCONHC_6H_4SH$ and $(NEt_4^+)(4\text{-}Ph_3CCONHC_6H_4S^-)$, exhibit an NH band at 3410, 3409, and 3409 cm^{-1} and a CO band at 1677, 1683, and 1675 cm^{-1}, respectively. These ν(NH) values exhibit somewhat similar values because the intramolecular NH···S hydrogen bond cannot form in 4-acylaminobenzenethiol derivatives.

The IR data in the amide region ν(NH) and ν(C═O) bands in the solid state for the platinum and palladium complexes, free ν(NH) and ν(C═O) bands of the corresponding thiol

---

(41) Patel, D. J. *Biochemistry* **1973**, *12*, 667−676.
(42) Patel, D. J. *Biochemistry* **1973**, *12*, 677−688.
(43) Gellman, S. H.; Dado, G. P.; Liang, G. B.; Adams, B. R. *J. Am. Chem. Soc.* **1991**, *113*, 1164−1173.
(44) Onoda, A.; Yamada, Y.; Takeda, J.; Nakayama, Y.; Okamura, T.; Doi, M.; Yamamoto, H.; Ueyama, N. *Bull. Chem. Soc. Jpn.* **2004**, *77*, 321−329.

Table 3. IR Spectral Data (cm^{-1}) for M(bpy)(bis)thiolates (M = Pt^{II}, Pd^{II}) Complexes and Related Compounds in Chloroform (10 mM) and in the Solid State

	chloroform		solid state	
compound	ν(NH)	ν(CO)	ν(NH)	ν(CO)
[Pt(bpy)(S-2-$Ph_3CCONHC_6H_4$)$_2$] (**1**)	3288, 3325	1673	3278	1675
[Pt(bpy)(S-4-$Ph_3CCONHC_6H_4$)$_2$] (**2**)	3410	1677	3404	1681
[Pt(bpy)(S-2-*t*-$BuNHCOC_6H_4$)$_2$] (**3**)	3305	1636, 1648	3241, 3298	1634, 1648
[Pd(bpy)(S-2-$Ph_3CCONHC_6H_4$)$_2$] (**4**)	3281, 3323	1672	3280, 3333	1675
2-$Ph_3CCONHC_6H_4SH$	3343	1685	3348	1696
(NEt_4^+)(2-$Ph_3CCONHC_6H_4S^-$)	3150	1654	3140	1644
4-$Ph_3CCONHC_6H_4SH$	3409	1683	3398	1681
(NEt_4^+)(4-$Ph_3CCONHC_6H_4S^-$)	3409	1675	3411	1675
2-*t*-$BuNHCOC_6H_4SH$	3431	1658	3303	1632
(NEt_4^+)(2-*t*-$BuNHCOC_6H_4S^-$)	3153	1618	3154	1618

Table 4. IR Shift $\Delta\nu$(NH) of the Amide NH Band by the NH···S Hydrogen Bond in Various Metal Complexes with 2-(Acylamino)benzenethiolate Ligands (SAr)

compound	$\Delta\nu$(NH)/cm^{-1}	ref
[Pt(bpy)(SAr)$_2$]^a	−55	this work
[Pd(bpy)(SAr)$_2$]^a	−62	this work
(NEt_4)[Cu^I(SAr)$_3$]^b	−171	34
(NEt_4)$_2$[Co^{II}(SAr)$_4$]^b	−114	21
(NEt_4)$_2$[Cd^{II}(SAr)$_4$]^b	−126	
(NEt_4)[Mo^{V}O(SAr)$_4$]^c	−67	32
[Hg^{II}(SAr)$_2$]^b	−52	35
[Fe^{III}(OEP)(SAr)]^d	−66	29
[Ga^{III}(OEP)(SAr)]^b	−143	33

[a] S-2-$Ph_3CCONHC_6H_4$. [b] S-2-*t*-$BuCONHC_6H_4$. [c] S-2-$CH_3CONHC_6H_4$. [d] S-2-$CF_3CONHC_6H_4$.

compounds, and the shift values are all summarized in Table 3. The thiol forms, 2-$Ph_3CCONHC_6H_4SH$ and 4-$Ph_3CCONHC_6H_4SH$, in the solid state exhibit NH bands at 3348 and 3398 cm^{-1} and CO bands at 1696 and 1681 cm^{-1}, respectively. These bands ν(NH) and ν(C=O) in the solid state are similar to those in solution and different from those of 2-*t*-$BuNHCOC_6H_4SH$. This result suggests that these compounds do not have an intermolecular NH···O=C hydrogen bond in the solid state as does 2-*t*-$BuNHCOC_6H_4SH$.[40] Complexes **1** and **4** exhibit NH bands at 3278, 3280, and 3333 cm^{-1}, and CO bands at 1675 and 1675 cm^{-1}, respectively. The $\Delta\nu$(NH) values for **1** and **4** can be estimated to be −70 and −68 cm^{-1} when the stretching of the free NH in the thiol compound is employed as a standard, and the shifts are ascribed to an NH···S hydrogen bond as well as occurring in solution. These $\Delta\nu$(NH) values are smaller than that of the thiolate anion, (NEt_4^+)(2-$Ph_3CCONHC_6H_4S^-$) (3140 cm^{-1}). This finding suggests that these NH···S hydrogen bonds are weak, as would be expected from the X-ray analysis. Complex **3** exhibits NH bands at 3241 and 3298 cm^{-1} and CO bands at 1634 and 1648 cm^{-1}. The two separate NH and CO bands are tentatively assigned to those with two distinct NH···S hydrogen bonds detected by the X-ray analysis. Complex **2** exhibits an NH band at 3404 cm^{-1} and a CO band at 1681 cm^{-1}, without a hydrogen bond.

The $\Delta\nu$(NH) values in the platinum complex **1**, the palladium complex **4**, and the reported complexes are summarized in Table 4. As compared to other metal complexes, the relatively small $\Delta\nu$(NH) values in complexes **1** and **4** are similar to each other as the Mo(V),[32] Hg(II),[35] or Fe(III)[29] complex and are ascribed to a weak interaction between NH and S pπ against the strongly covalent Pt−S and Pd−S bonds.

UV−Visible Spectra. The absorption spectra of the platinum complexes [Pt(bpy)(S-2-$Ph_3CCONHC_6H_4$)$_2$] (**1**) and [Pt(bpy)(S-4-$Ph_3CCONHC_6H_4$)$_2$] (**2**) at 298 K exhibit a broad asymmetric absorption band with medium intensity in the visible region (400−600 nm) (Figure 4). This lowest energy absorption band at 530 nm in Pt(bpy)(SC_6H_5)$_2$ is assigned as the transition from the HOMO composed of thiolate(π)/S(p)/Pt(d) orbitals to the LUMO largely localized on the π* (bipyridine) orbital and shifts to a lower energy level with an increase of the thiolate ligand donor ability.[2] The lowest energy absorption band in complex **2** is detected at 537 nm (ϵ = 1020 M^{-1} cm^{-1}), which is only slightly shifted as compared to that in Pt(bpy)(SC_6H_5)$_2$ (530 nm, ϵ = 2140 M^{-1} cm^{-1}).[7] Because the electronic effect of the amide group at the 2- or 4-position of the benzene ring is known not to be significant for organic disulfide molecules,[45] that of acylamino group in these complexes is not significant. However, this band in complex **1** is detected at 488 nm (ϵ = 2410 M^{-1} cm^{-1}), consistent with a significant shift to higher energy. In the case of the Fe(II), Co(II),[21] Mo(V), and Mo(IV)[32] complexes, the local electron-withdrawing ability of the amide group through the NH···S hydrogen bond results in a decrease in the electron density of S(pπ). Consequently, this finding suggests that the intramolecular NH···S hydrogen bond decreases the electron density of S(pπ) coordinated to platinum in this case and the lowest energy absorption band largely shifts to a higher energy level.

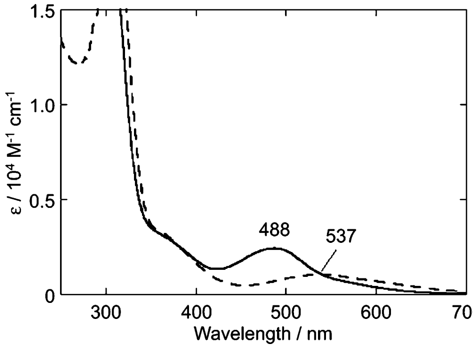

Figure 4. Electronic absorption spectra of [Pt(bpy)(S-2-$Ph_3CCONHC_6H_4$)$_2$] (**1**) (—) and [Pt(bpy)(S-4-$Ph_3CCONHC_6H_4$)$_2$] (**2**) (− − −) in tetrahydrofuran at 298 K.

---

(45) Jaffe, H. H. *Chem. Rev.* **1953**, *53*, 191−261.

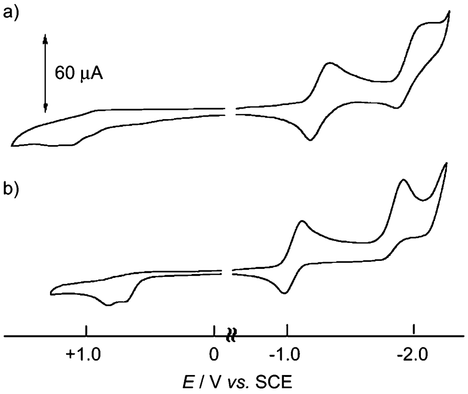

Figure 5. Cyclic voltammograms of a 1.0 mM solution of (a) [Pt(bpy)(S-2-$Ph_3CCONHC_6H_4)_2$] (**1**) and (b) [Pt(bpy)(S-4-$Ph_3CCONHC_6H_4)_2$] (**2**) in tetrahydrofuran at room temperature. Scan rate: 100 mV/s.

Table 5. Cyclic Voltammetric Data of Pt(bpy)(Bis)thiolates Complexes and Related Compounds[a]

compound	$E_{p,a}$/V	$E_{1/2}^{0/-}$/V	$E_{1/2}^{-/2-}$/V
[Pt(bpy)(S-2-$Ph_3CCONHC_6H_4)_2$] (**1**)	+1.04	−1.20	−1.84
[Pt(bpy)(S-4-$Ph_3CCONHC_6H_4)_2$] (**2**)	+0.69(sh), +0.79	−1.05	−1.88[c]
[Pt(bpy)($SC_6H_5)_2$][b]	+0.80	−1.14	−1.79
[Pt(bpy)Cl_2][b]	+1.24	−1.07	−1.73

[a] Measured in tetrahydrofuran (0.2 M NBu_4PF_6) versus SCE at 298 K and a scan rate of 100 mV/s. [b] From ref 7. [c] Irreversible. Cathodic peak potential.

Electrochemical Properties. The cyclic voltammograms of the platinum complexes [Pt(bpy)(S-2-$Ph_3CCONHC_6H_4)_2$] (**1**) and [Pt(bpy)(S-4-$Ph_3CCONHC_6H_4)_2$] (**2**) in tetrahydrofuran are shown in Figure 5. The redox potentials are listed in Table 5. The first reduction is a one-electron process, which is reversible for complexes **1** and **2**. The value of the first reduction potential is largely unaffected by the nature of the thiolate and is close to the value of the first reduction for Pt(bpy)Cl_2. This suggests that the LUMO is mainly localized on the bpy ligand.[2] The values of the second reduction potentials of complexes **1** and **2** are very similar to each other and are close to that for Pt(bpy)Cl_2 (Table 5). These second reductions are a quasi-reversible process.

On the other hand, the oxidation is irreversible for complexes **1** and **2**. The value of the oxidation potential is largely affected and in a manner different from that of the reduction potential because the HOMO is mainly composed of thiolate (π)/S(p)/Pt(d) orbital. The value of the oxidation potential for complexes **1** and **2** manifests at +1.04 and +0.79 V (versus SCE), respectively. The value for complex **2** is the same as that for Pt(bpy)($SC_6H_5)_2$ (+0.80 V versus SCE).[7] In contrast, the value for complex **1** shifts to largely positive ($\Delta E = +0.2$ V). The observed remarkable positive shift is attributed to the intramolecular NH···S hydrogen bond. The contribution of NH···S hydrogen bonding to the positive shift of redox potential was proposed for native metalloproteins as early as 1975,[36,46] and this hypothesis is supported by the model complexes. The oxidation potential $E_{p,a}$ values shift very positively with decreasing donor capacity of the thiolate ligand. Consequently, the intramolecular NH···S hydrogen bond decreases the electron density of S(pπ) coordinated to platinum as well as the result of UV−visible spectra.

Conclusions

2-(Acylamino)benzenethiolate and 2-(alkylcarbamoyl)-benzenethiolate complexes of Pt(bpy) and Pd(bpy) having an intramolecular NH···S hydrogen bond, Pt(bpy)(S-2-$Ph_3CCONHC_6H_4)_2$ (**1**) and Pt(bpy)(S-2-*t*-$BuNHCOC_6H_4)_2$ (**3**), were synthesized, and their crystal structures were determined. The presence of a weak NH···S hydrogen bond in both complexes and Pd(bpy)(S-2-$Ph_3CCONHC_6H_4)_2$ (**4**) is established by the observation of the temperature coefficients of the NH signal in the ^{1}H NMR spectra and the shifted NH stretching of the amide groups in the IR spectra in chloroform and in the solid state. The lowest energy absorption band in complex **1** shows the high-energy shift by the effect of the NH···S hydrogen bond. In addition, the oxidation potential in complex **1** shows the positive shift with a decrease of the electron density for S(pπ) coordinated to platinum correlated to the HOMO due to the NH···S hydrogen bond.

Experimental Section

Materials. All operations were performed under an argon atmosphere. All solvents were dried and distilled under argon before use. 2,2′-Dithiobis(*N*-phenyl-2,2,2-triphenylacetamide) and 2,2′-dithiobis[*N*-(1,1-dimethyl ethyl)benzamide] were prepared by literature procedures. The syntheses of 2-triphenylacetylaminobenzenethiol, tetraethylammonium 2-triphenylacetylaminobenzenethiolate, 4-triphenylacetylaminobenzenethiol, and tetraethylammonium 4-triphenylacetylaminobenzenethiolate were carried out using the same previously reported procedure.[40]

Synthesis of [Pt(bpy)(S-2-$Ph_3CCONHC_6H_4)_2$] (1). Bis[2-(triphenylacetylamino)phenyl] disulfide (79 mg, 0.10 mmol) and NBu_4BH_4 (64 mg, 0.25 mmol) were suspended in tetrahydrofuran (5 mL). To the solution was added dropwise Pt(bpy)Cl_2 (42 mg, 0.1 mmol) in dimethyl sulfoxide (DMSO, 3 mL). The yellow solution changed to dark brown. Stirring was continued for an hour at room temperature. The reaction mixture was acidified with HCl aqueous solution and extracted with chloroform. The solution was washed with 2% HCl aqueous solution, NaCl-saturated aqueous solution, saturated $NaHCO_3$ aqueous solution, and NaCl-saturated aqueous solution. The organic layer was dried with anhydrous sodium sulfate and concentrated under pressure. The obtained brown powder was washed diethyl ether and dried under vacuo. The crude product was reprecipitated from hot methanol and recrystallized from acetone. Yield 53.7 mg (47%). mp 175 °C. Anal. Calcd for $C_{62}H_{48}N_4O_2PtS_2 \cdot CH_3OH$: C, 64.54; H, 4.47; N, 4.78. Found: C, 64.54; H, 4.25; N, 4.81. ESI-MS: *m*/*z* 1163 [M + Na]$^+$. ^{1}H NMR (chloroform-*d*$_1$): δ 9.33 (dd, 2H), 8.74 (s, 2H), 8.10 (td, 2H), 8.00−8.02 (m, 4H), 7.46 (td, 2H), 7.40 (dd, 2H), 7.28 (m, 12H), 7.15 (m, 12H), 7.06 (tt, 6H), 6.83 (td, 2H), 6.51 (td, 2H).

Synthesis of [Pt(bpy)(S-4-$Ph_3CCONHC_6H_4)_2$] (2). The complex was synthesized by the same method described above for the synthesis of [Pt(bpy)(S-2-$Ph_3CCONHC_6H_4)_2$]. The crude complex was precipitated from acetone. Yield 71%. mp > 250 °C. ESI-MS: *m*/*z* 1163 [M + Na]$^+$. ^{1}H NMR (chloroform-*d*$_1$): δ 9.85 (d, 2H), 8.07 (td, 2H), 8.01 (d, 2H), 7.54 (dt, 4H), 7.51 (td, 2H), 7.17−7.34 (m, 30H), 6.99 (4H, dt).

Synthesis of [Pt(bpy)(S-2-*t*-$BuNHCOC_6H_4)_2$] (3). The complex was synthesized by the same method described above for the

---

(46) Carter, C. W., Jr. *J. Biol. Chem.* **1977**, *252*, 7802−7811.

Table 6. Crystallographic Data for [Pt(bpy)(S-2-$Ph_3CCONHC_6H_4$)$_2$] (**1**) and [Pt(bpy)(S-2-*t*-BuNHCOC$_6H_4$)$_2$] (**3**)

	1·2$(CH_3)_2CO$·H_2O	**3**·$(CH_3)_2CO$
chemical formula	$C_{68}H_{62}N_4O_5S_2Pt$	$C_{35}H_{42}N_4O_3S_2Pt$
formula weight	1274.47	825.95
T/K	200(1)	200(1)
crystal system	monoclinic	monoclinic
lattice parameter		
a/Å	16.522(4)	30.881(4)
b/Å	19.518(5)	14.258(2)
c/Å	17.644(3)	19.371(2)
β/deg	95.624(9)	124.109(6)
V/Å^3	5662(2)	7061(1)
Z	4	8
space group	$P2_1/n$ (No. 14)	$C2/c$ (No. 15)
D_{calc}/g cm^{-3}	1.495	1.559
μ/cm^{-1}	25.99	41.31
reflns collected	38 690	32 649
ind reflns (R_{int})	12 689 (0.106)	8028 (0.031)
R_1 for $I > 2\sigma(I)$	0.0460	0.0219
wR_2 for all data	0.0545	0.0504

synthesis of [Pt(bpy)(S-2-$Ph_3CCONHC_6H_4$)$_2$]. The crude complex was precipitated from acetone. Yield 80%. mp 200 °C. Anal. Calcd for $C_{32}H_{36}N_4O_2PtS_2$: C, 50.05; H, 4.73; N, 7.30. Found: C, 49.73; H, 4.60; N, 7.31. ESI-MS: *m/z* 634.1 [M + Na]$^+$. ^{1}H NMR (chloroform-*d*$_1$): δ 9.77 (d, 2H), 8.14 (td, 2H), 8.09 (d, 2H), 7.92 (dd, 2H), 7.59 (td, 2H), 7.53 (dd, 2H), 7.40 (s, 2H), 6.96 (td, 2H), 6.86 (td, 2H), 1.35 (s, 18H).

Synthesis of [Pd(bpy)(S-2-$Ph_3CCONHC_6H_4$)$_2$] (4). To a suspension of Pd(bpy)Cl_2 (47 mg, 0.14 mmol) and 2-triphenylacetylaminobenzenethiol (112.3 mg, 0.28 mmol) in acetonitrile (12 mL) was added triethylamine (40 μL). The solid slowly turned dark red. After the mixture was stirred overnight, the solid was filtered off, washed with methanol, and suction dried. The crude complex was recrystallized from tetrahydrofuran. Yield 65%. mp 170 °C. Anal. Calcd for $C_{62}H_{48}N_4O_2PdS_2$·1.5H_2O: C, 69.04; H, 4.77; N, 5.19. Found: C, 68.96; H, 4.76; N, 5.03. ESI-MS: *m/z* 1073 [M + Na]$^+$. ^{1}H NMR (chloroform-*d*$_1$): δ 8.77 (d, 2H), 8.75 (s, 2H), 8.03 (dd, 2H), 7.93−8.00 (m, 4H), 7.39 (td, 2H), 7.35 (dd, 2H), 7.22 (m, 12H), 7.08 (m, 12H), 6.98 (tt, 6H), 6.80 (td, 2H), 6.44 (td, 2H).

Physical Measurements. ^{1}H NMR spectra was obtained on a JEOL GSX-400 spectrometer in chloroform-*d*$_1$ or acetonitrile-*d*$_3$ solution at 303 K. Tetramethylsilane (TMS) was used as the internal reference for proton resonance. IR spectra were taken on a Jasco FT/IR-8300 spectrometer. Samples were prepared as chloroform-*d*$_1$ solutions or KBr pellets. ESI-mass spectrometric analyses were performed on a Finniganmat LCQ-MS instrument in methanol or acetonitrile. Absorption spectra were recorded on a Shimadzu UV-3100PC spectrophotometer using a 1-cm cell. The cyclic voltammograms were recorded on a BAS 100B/W instrument with a three-electrode system consisting of a glassy carbon working electrode, a platinum-wire counter electrode, and a saturated calomel electrode (SCE). The scan rate was 100 mV/s. The sample concentration was 1 mM in tetrahydrofuran, containing 0.2 M NBu_4BF_4 as supporting electrolyte. Potentials were determined at room temperature versus SCE as a reference.

Structure Determinations. The data collections for Pt(bpy)(S-2-$Ph_3CCONHC_6H_4$)$_2$ (**1**) and Pt(bpy)(S-2-*t*-BuNHCOC$_6H_4$)$_2$ (**3**) were carried out on a Rigaku RAXIS-RAPID Imaging Plate diffractometer using graphite-monochromated Mo Kα radiation (λ = 0.71075 Å) at 200 K. The basic crystallographic parameters for **1** and **3** are listed in Table 6. The structures were solved by direct method with SIR92[47] and expanded using Fourier techniques. The absorption correction for both complexes was performed by multiscan method. All non-hydrogen atoms were refined anisotropically by the full-matrix least-squares method on F^2 using SHELXL-97.[48] Hydrogen atoms were not refined. In complex **3**, one thiophenol ligand and a solvent acetone molecule are disordered into two positions with site occupancy factors of each 0.500. All calculations were carried out on SGI workstation using the teXsan[49] crystallographic software package of the Molecular Structure Corp.

Molecular Orbital Calculations. Density functional theory (DFT) calculations at Becke's three-parameter hybrid functional with the correlation functional of Lee, Yang, and Parr (B3LYP) level[50−52] for Pt(bpy)(S-2-*t*-BuCONHC$_6H_4$)$_2$ were carried out on the basis of the crystal structure of Pt(bpy)(S-2-$Ph_3CCONHC_6H_4$)$_2$ (**1**) and with the assumption of an idealized coplanar structure between amide plane and thiophenol plane using the Gaussian 03 system of programs.[53] The effective core potentials (ECP) of Hay and Wadt with double-ζ valence basis set (LanL2DZ)[54] were used.

Acknowledgment. This work was supported by a Grant-in-Aid for Scientific Research on Priority Area (A) (No. 12304040) from the Ministry of Education, Culture, Sports, Science, and Technology, Japan. M.K. expresses his special thanks for the center of excellence (21COE) program "Creation of Integrated EcoChemistry of Osaka University".

Supporting Information Available: X-ray crystallographic data in CIF format. This material is available free of charge via the Internet at http://pubs.acs.org.

IC0490167

---

(47) Altomare, A.; Cascarano, G.; Giacovazzo, G.; Guagliardi, A. SIR92-A program for crystal structure solution. *J. Appl. Crystallogr.* **1993**, *27*, 435.

(48) Sheldrick, G. M. *SHELXL-97: Program for the Refinement of Crystal Structures*; University of Gottingen: Gottingen, Germany, 1997.

(49) *teXsan: Crystal Structure Analysis Program*; Molecular Corp.: The Woodlands, TX, 1985 and 1992.

(50) Becke, A. D. *Phys. Rev. A* **1988**, *38*, 3098−3100.

(51) Becke, A. D. *J. Chem. Phys.* **1993**, *98*, 5648−5652.

(52) Lee, C.; Yang, W.; Parr, R. G. *Phys. Rev. B* **1988**, *37*, 785−789.

(53) Frisch, M. J.; Trucks, G. W.; Schlegel, H. B.; Scuseria, G. E.; Robb, M. A.; Cheeseman, J. R.; Montgomery, J. A., Jr.; Vreven, T.; Kudin, K. N.; Burant, J. C.; Millam, J. C.; Iyengar, S. S.; Tomasi, J.; Barone, V.; Mennucci, B.; Cossi, M.; Scalmani, G.; Rega, N.; Petersson, G. A.; Nakatsuji, H.; Hada, M.; Ehara, M.; Toyota, K.; Fukuda, R.; Hasegawa, J.; Ishida, M.; Nakajima, T.; Honda, Y.; Kitao, O.; Nakai, H.; Klene, M.; Li, X.; Knox, J. E.; Hratchian, H. P.; Cross, J. B.; Adamo, C.; Jaramillo, J.; Gomperts, R.; Stratmann, R. E.; Yazyev, O.; Austin, A. J.; Cammi, R.; Pomelli, C.; Ochterski, J. W.; Ayala, P. Y.; Morokuma, K.; Voth, G. A.; Salvador, P.; Dannenberg, J. J.; Zakrzewski, V. G.; Dapprich, S.; Daniels, A. D.; Strain, M. C.; Farkas, O.; Malick, D. K.; Rabuck, A. D.; Raghavachari, K.; Foresman, J. B.; Ortiz, J. V.; Cui, Q.; Baboul, A. G.; Clifford, S.; Cioslowski, J.; Stefanov, B. B.; Liu, G.; Liashenko, A.; Piskorz, P.; Komaromi, I.; Martin, R. L.; Fox, D. J.; Keith, T.; Al-Laham, M. A.; Peng, C. Y.; Nanayakkara, A.; Challacombe, M.; Gill, P. M. W.; Johnson, B.; Chen, W.; Wong, M. W.; Gonzalez, C.; Pople, J. A. *Gaussian03*, revision B.5; Gaussian, Inc.: Pittsburgh, PA, 2003.

(54) Hay, P. J.; Wadt, W. R. *J. Chem. Phys.* **1985**, *82*, 299−310.